

Received 10 February 2023, accepted 9 March 2023, date of publication 15 March 2023, date of current version 21 March 2023.

Digital Object Identifier 10.1109/ACCESS.2023.3257431

RESEARCH ARTICLE

Sustainable Heavy Goods Vehicle Electrification Strategies for Long-Haul Road Freight Transportation

G. ROHITH¹, K. B. DEVIKA², PRATHYUSH P. MENON²,
AND SHANKAR C. SUBRAMANIAN³, (Senior Member, IEEE)

¹Orbital Astronautics, OX14 4SA Oxfordshire, U.K.

²Faculty of Environment, Science and Economy, University of Exeter, EX4 4QF Exeter, U.K.

³Department of Engineering Design, Indian Institute of Technology Madras, Chennai 600036, India

Corresponding author: K. B. Devika (D.Koonthalakadu-baby@exeter.ac.uk)

The work of Prathyush P. Menon was supported in part by the industrial project - A34 Catenary Cable Project (ID-969859), funded by City Science, Exeter, U.K.

ABSTRACT Even though diesel-powered Heavy Goods Vehicles (HGVs) are major contributors of greenhouse gas emission, HGV electrification is still in its infancy owing to various challenges. Costlier and heavier batteries and lack of charging infrastructure along long routes are the major bottlenecks in the realisation of HGV electrification for long-haul freight transportation. In this regard, adopting technologies that can make HGV electrification viable is vital to aid the transportation sector decarbonisation. Benefiting from approaches such as the use of overhead catenary power, and conforming to operate in a platoon formation, it would be possible to considerably reduce the cost of HGV electrification and make it economically feasible. Utilising overhead catenary infrastructure would result in requiring economical charging infrastructure, shorter charging cycles, and smaller batteries, while not compromising on the overall payload of HGVs. HGVs in platoon formation result in energy consumption reduction and increased traffic throughput. This paper investigates the benefits of using overhead catenary-powered electric HGVs for freight transportation and also explores the advantages associated with electric HGV platoon formations on the same. The feasibility analysis has been done with the support of close to real physics-based electric HGV models on realistic operating scenarios adopting an in-service highway drive cycle. From the analysis, electric HGV platooning using overhead catenary as the power source was found to be economical with $\approx 10.4\%$ reduction in electricity cost when compared to without platooning while devising electrification strategies for long-haul freight transportation.

INDEX TERMS Battery electric vehicle, catenary infrastructure, decarbonisation, energy savings, electrification, freight transportation, heavy goods vehicle, platooning, sustainable transportation.

I. INTRODUCTION

A significant challenge that the world faces today is mitigating climate change. Decarbonising the energy and transport sector is crucial in addressing this challenge. According to the Transport and Environment Statistics 2021 Annual report [1], the UK energy sector has been successfully contributing towards decarbonisation for the last 20 years. However, the

The associate editor coordinating the review of this manuscript and approving it for publication was Shaohua Wan.

contribution from the transport sector has been consistent over the period and remains one of the major contributors to greenhouse gas emissions. In 2019, the transport sector alone was accountable for 27% of the UK's total emissions, of which 91% were from road vehicles and 18% of that was from Heavy Good Vehicles (HGVs). The percentage is colossal, and heavy vehicles contribute only 5% of the total road vehicle miles travelled with the UK [1], making it more formidable. Similar numbers can be found for India, where HGVs, amounting to approximately 5% of total vehicle stock,

contribute towards 43% of total transport sector greenhouse gas emissions [2]. While considering the global statistics on sector vice contribution to greenhouse gas emission too, HGVs reflect a disproportionate contribution, representing 9% of global vehicle stock, however, causing around 40% of the total greenhouse gas emissions [3]. The automotive research community has given due importance to these disproportionate statistics and is working towards developing decarbonisation strategies for heavy vehicle operations because the current and future freight movement is highly dependent on HGVs.

Many decarbonisation policies have been proposed to realise sustainable freight transportation strategies. Vehicle level improvisations such as reducing aerodynamic and rolling resistance forces through improved vehicle body and tyre design and improving the efficiency of the propulsion drive-line have been investigated for enhanced heavy vehicle fuel efficiency and thereby reduced emissions [4], [5]. Use of alternative fuels, high-capacity articulated vehicles, and optimal planning of operating routes are some of the other strategies being explored for clean and sustainable heavy vehicle operation [6], [7].

Electrification of heavy vehicle operation is being viewed as the potential solution towards complete decarbonisation of the freight transportation sector [8]. Even though carbon footprints from electric energy generation are still a matter of concern, from a tailpipe emission perspective, electric HGVs could be considered as “fully decarbonised” [9]. Among HGV electrification strategies, hydrogen fuel cell-based operation has gained significant research interest recently [10]. However, infrastructure costs for hydrogen generation and the need for large storage tanks for liquid or gaseous hydrogen are the major bottlenecks of this technology for HGV electrification, primarily when used for long-haul freight transportation. Plug-in battery electric vehicle technology is another commonly discussed method for HGV electrification. However, when used for freight transportation, these vehicles would require high capacity/bigger batteries to complete long-haul routes. Moreover, deployment of plug-in battery HGVs for long routes requires sufficient charging infrastructure along the routes [11]. Using bigger batteries to increase the range of operation could reduce the HGVs’ cargo capacity and increase the total cost of ownership [12]. The long idling period during battery charging from static charging stations would also reduce the overall efficiency of the freight transportation [13]. A recent study [14] claims that using recent innovations in battery and fast charging technology, battery HGVs could potentially lead to cost-effective long-haul freight transportation.

An alternate way to improve the practical utility of battery HGVs for long-haul freight movement is to adopt the electric highway technology. In an electric highway, unlike plugging in the electric HGVs to static charging stations and idling while charging, it is possible to power/dynamically charge them from the electric grid either wireless [15], or through an overhead catenary infrastructure [16]. This

dynamic charging opportunity, deployed along highway segments through catenary-pantograph interaction, enables electricity to be directly transmitted to the electric motor and/or charge the battery on board. The online availability of electricity and the dynamic charging capability could result in the long-range operation of battery electric HGVs with significantly small-sized batteries, leading to increased cargo capacity and reduced idling time [17]. However, the realisation of electric highways for this purpose involves high infrastructure costs and demands standardisation of HGV technology. Commissioning of overhead catenary infrastructure for highway electrification across wider regions (e.g., all over the UK) is also required to make this system profitable, considering the initial infrastructure investment. This dynamic charging system has already been demonstrated as trolleybuses powered by overhead catenary lines deployed in many cities [18]. Significant research demonstrating the capability of this technology for economical freight transportation using electric HGVs has been going on in Germany, and Sweden [19], [20]. This technique has been studied for its feasibility in the UK highways too [21], [22]. In the current study, the feasibility of HGV electrification through overhead catenary lines has been analysed closely with the support of a detailed physics-based model of heavy vehicles.

Vehicle platooning is a concept that has gained significant research interest and has been well studied as it could result in better fuel economy during vehicular operation [23], [24]. In a platoon, vehicles travel one behind the other, and very close to each other, thus reducing the aerodynamic drag force on them. During high-speed cruising of HGVs, a significant amount of energy is utilised to overcome the aerodynamic drag force [25], [26]. Hence, platoon formation of HGVs has been considered a potential policy to be adopted during highway operation, where the vehicles cruise at high speed to improve fuel economy. A platoon of electric HGVs could reduce the energy usage from the energy source (battery/overhead line), thus leading to an improved range of operations. Hence, an in-depth analysis of electric HGV operation in platoon formations, mainly when powered by the overhead catenary infrastructure, is being investigated and discussed in this paper.

II. ELECTRIC HGV DYNAMICS

To emulate actual vehicle operating conditions, a detailed electric HGV dynamics model encompassing factors such as resistive forces, tyre model, normal forces, wheel slip and wheel dynamics are used for the performance analysis. The electric HGV dynamic model considering the longitudinal motion of the vehicle has been developed. The position and speed dynamics of vehicle can be represented as:

$$\begin{aligned}\dot{x}(t) &= v(t), \\ \dot{v}(t) &= \Omega(v(t), \tau_v(t)),\end{aligned}\quad (1)$$

where, $v(t)$ and $\tau_v(t)$ represent the longitudinal speed and drive/brake torque of the vehicle. Here, $\Omega(v(t), \tau_v(t))$ is a

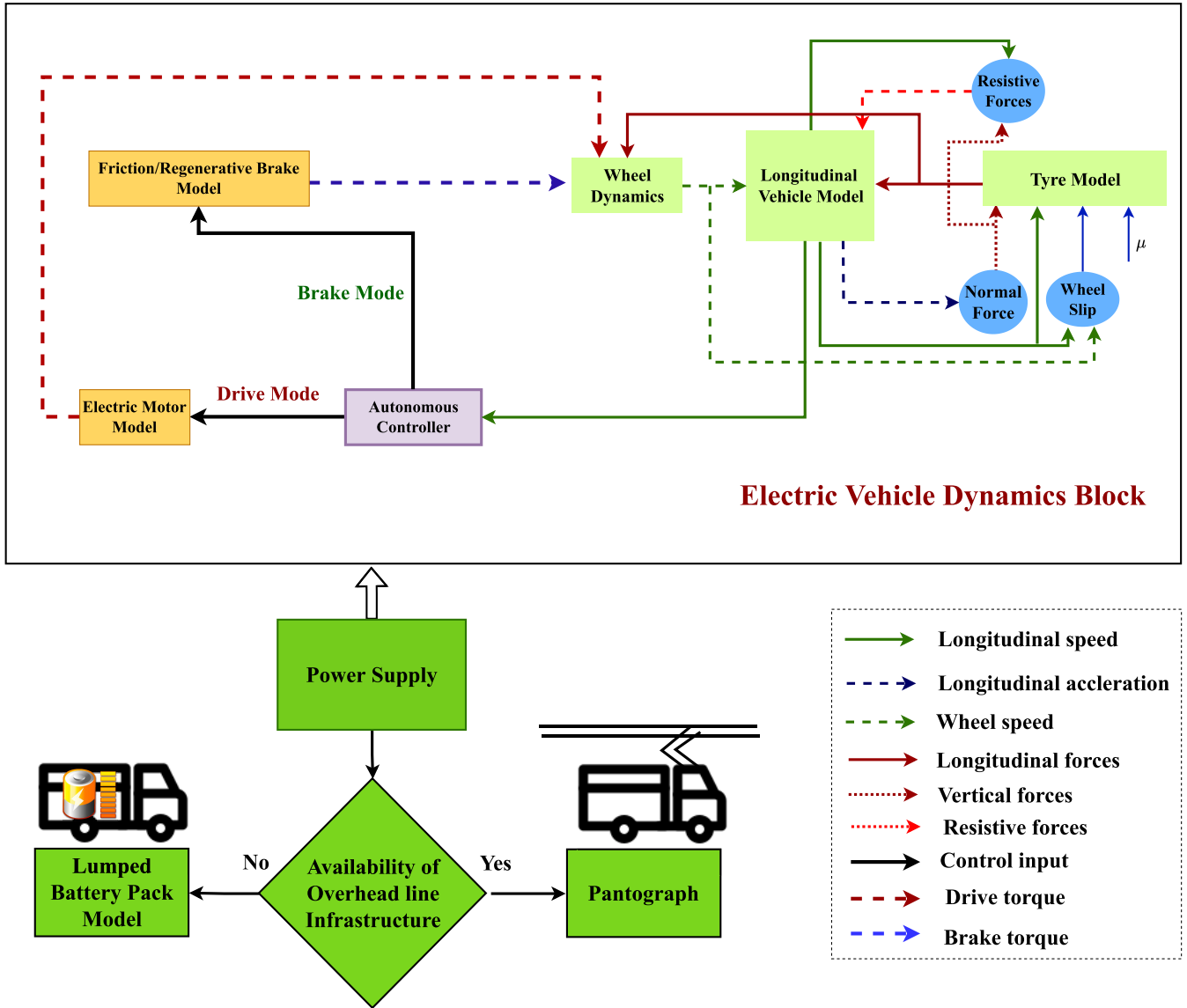


FIGURE 1. A detailed schematic of the electric HGV model with autonomous controller and battery/overhead line as power supply.

nonlinear function in $v(t)$ and $\tau_v(t)$ that can be expressed as

$$\Omega(v(t), \tau_v(t)) = \frac{1}{m_v} (F_{xfv}(\lambda_{fv}(t)) + F_{xrv}(\lambda_{rv}(t)) - F_{Rv}(t)), \quad (2)$$

where, m_v is the mass of the vehicle, $F_{xfv}(\lambda_{fv}(t))$ and $F_{xrv}(\lambda_{rv}(t))$ represent the longitudinal forces at the front and rear tyre-road interface respectively, and $\lambda_{fv}(t)$ and $\lambda_{rv}(t)$ represent the longitudinal slip ratios of front and rear wheels, respectively. They are calculated as,

$$\lambda_{fv}(t) = \frac{v(t) - r \omega_{fv}(t)}{v(t)}, \quad \lambda_{rv}(t) = \frac{v(t) - r_i \omega_{rv}(t)}{v(t)}, \quad (3)$$

where, r is the tyre radius.

The wheel dynamics is given by,

$$\begin{aligned} \dot{\omega}_{fv}(t) &= \frac{1}{I_f} (\tau_{fv}(t) - r F_{xfv}(\lambda_{fv}(t))), \\ \dot{\omega}_{rv}(t) &= \frac{1}{I_r} (\tau_{rv}(t) - r F_{xrv}(\lambda_{rv}(t))), \end{aligned} \quad (4)$$

where, $\omega_{fv}(t)$ and $\omega_{rv}(t)$ are the angular speeds of front and rear wheels, respectively, I_f and I_r are the moment of inertia of front and rear wheels respectively, $\tau_{fv}(t)$ and $\tau_{rv}(t)$ are the transmitted torques to the front and rear wheels, respectively.

The longitudinal force components, $F_{xfv}(\lambda_{fv}(t))$ and $F_{xrv}(\lambda_{rv}(t))$, are computed using the Magic Formula (MF) tyre model proposed by [27], since the MF tyre model gives a good representation of forces acting on the tyre-road interface for a wide range of operating conditions. The magnitude of the longitudinal force depends on the longitudinal slip

ratios presented by equation (3) and the normal forces at the tyre-road interface. The normal forces at the front and rear tyre-road interface for are given by,

$$\begin{aligned}
 F_{zf_v}(t) &= \frac{m_v g l_{rv} \cos(\theta) - F_{av}(t) h_a - m_v a(t) h_{cg}}{L} \\
 &\quad - \frac{m_v g h_{cg} \sin(\theta)}{L}, \\
 F_{zr_v}(t) &= \frac{m_v g l_{fv} \cos(\theta) + F_{av}(t) h_a + m_v a(t) h_{cg}}{L} \\
 &\quad + \frac{m_v g h_{cg} \sin(\theta)}{L}, \tag{5}
 \end{aligned}$$

where, $a(t) = \ddot{x}(t)$ is the longitudinal acceleration, h_{cg} is the height of the center of gravity (C.G.) of the vehicle, h_a is the height of the location at which the equivalent aerodynamic force acts, θ represents the road inclination, and l_{fv} and l_{rv} are the longitudinal distance of the front axle and rear axle from the C.G. of the vehicle, and $L = l_{fv} + l_{rv}$.

Now using the MF tyre model, the longitudinal forces at front and rear tyre-road interface are calculated as,

$$\begin{aligned}
 F_{xf_v}(\lambda_{xf_v}(t)) &= D_{xf} \sin \left(C_{xf} \tan^{-1} \left(B_{xf} \lambda_{xf}(t) \right. \right. \\
 &\quad \left. \left. - E_{xf} (B_{xf} \lambda_{xf}(t) - \tan^{-1} (B_{xf} \lambda_{xf}(t))) \right) \right) \\
 &\quad + S_{Vf}, \\
 F_{xr_v}(\lambda_{xr_v}(t)) &= D_{xr} \sin \left(C_{xr} \tan^{-1} \left(B_{xr} \lambda_{xr}(t) \right. \right. \\
 &\quad \left. \left. - E_{xr} (B_{xr} \lambda_{xr}(t) - \tan^{-1} (B_{xr} \lambda_{xr}(t))) \right) \right) \\
 &\quad + S_{Vr},
 \end{aligned}$$

where, $\lambda_{xf_v}(t) = \lambda_{fv}(t) + S_{Hf}$, $\lambda_{xr_v}(t) = \lambda_{rv}(t) + S_{Hr}$.

The MF model parameters, $B_{xf/r}$, $C_{xf/r}$, $D_{xf/r}$, $E_{xf/r}$, $S_{Hf/r}$, $S_{Vf/r}$, corresponding to front and rear tyre-road interface [28].

Now, $F_R(t)$ in equation (2) can be expressed as,

$$\begin{aligned}
 F_{Rv}(t) &= F_{av}(t) + R_{xf_v}(t) + R_{xr_v}(t) + F_{grad}(t) \\
 &= \rho a_f C_D \frac{v(t)^2}{2} + f(F_{zf_v}(t) + F_{zr_v}(t)) \\
 &\quad + m_v g \sin(\theta), \tag{6}
 \end{aligned}$$

where, $F_{av}(t)$ represents the force due to aerodynamic drag, R_{xf_v} and R_{xr_v} are the forces due to rolling resistance at the front and rear wheels, respectively, and F_{grad} represents the force component due to the road slope. The aerodynamic drag force is given by $F_{av}(t) = \rho a_f C_D \frac{v(t)^2}{2}$, where ρ is the air density, C_D represents the aerodynamic drag coefficient, and a_f represents the vehicle frontal area. The rolling resistance is characterised by the rolling resistance coefficient, f , and the normal forces at both front and rear tyre-road interface, $F_{zf_v}(t)$ and $F_{zr_v}(t)$, respectively.

A. MOTOR AND PNEUMATIC ACTUATOR MODELS

An electric vehicle uses an electric motor as a prime mover to provide the necessary drive/propulsion torque. In this work, an induction motor is used as the actuation mechanism and

represented using Equation (7). The same motor model in Equation (7) characterises the regenerative braking component. The transfer function representation of the motor model is given by,

$$P_m(s) = m_a \frac{V_{dc}}{2} e^{-\frac{T_{dm}s}{2}} \frac{K_m}{1 + \tau_m s}, \tag{7}$$

where, m_a is the modulation index of the inverter circuit, $\frac{V_{dc}}{2}$ is the inverter gain, T_{dm} is the PWM delay, K_m and τ_m represent the gain and time constant of the electric motor respectively. A detailed derivation of this transfer function is presented in [29].

During braking, the conventional friction brake system co-exists with the regenerative brake system to satisfy the braking force demands. In HGVs, traditionally, pneumatic brakes are used for this purpose. Practically, pneumatic brake response has significant delays due to factors such as compressibility of air, pipe lengths, valve response time, and delays in the pressure build-up in the brake chamber. These factors have been accommodated while modelling the brake system to have a close-to-real response. In this regard, Equation (8) is used to model the friction brake system dynamics.

Using Hardware in Loop experiments, the air brake system is characterised using a first order process with time delay transfer function as [30],

$$P(s) = \frac{1}{1 + \delta s} e^{-T_d s}, \tag{8}$$

where T_d represents the time delay and δ represents the time constant. The specific values for time constant (δ) and time delay (T_d) have also been experimentally obtained as $\tau_d = 260$ ms and $T_d = 45$ ms [30], and these values have been utilised in this study.

Cooperative use of friction and regenerative braking is necessary to have an optimum braking performance [31]. It is common to apply regenerative braking on the driven wheels only (rear wheels for the class of vehicles considered in this study) and friction braking on front and rear wheels. Series Cooperative Braking (SCB) and Parallel Cooperative Braking (PCB) are the most commonly used cooperative braking strategies [31]. In SCB, as the name indicates, regenerative and friction braking components are applied serially, one after another. Initially, regenerative braking is used, and when the brake force demand exceeds the maximum regenerative force, friction braking is applied on both front and rear wheels. In PCB, both regenerative and friction braking components are used parallelly.

$$\begin{aligned}
 F_{bf} &= F_{bf_{fric}}, \\
 F_{br} &= F_{br_{fric}} + F_{br_{regen}}, \tag{9}
 \end{aligned}$$

where F_{bf} and F_{br} represent the front and rear wheel braking forces, respectively, $F_{bf_{fric}}$ and $F_{br_{fric}}$ represent the friction brake force components of front and rear wheels, respectively, and $F_{br_{regen}}$ represents the regenerative braking force applied at the rear wheels.

The regenerative braking force is computed as a fraction of the total braking force and is applied to the driven wheels. Owing to less complex and easy to implement structure, this work adopts a PCB strategy to emulate regenerative braking.

$$F_{br_{regen}} = \gamma F_b, \quad (10)$$

where γ is the ratio of regenerative braking force to the total braking force. In this work the value of γ was chosen to be 0.1. Also, the distribution between front and rear braking forces follow a linear proportion, such that,

$$\frac{F_{bf}}{F_{br}} = \frac{\beta}{1 - \beta}, \quad (11)$$

where F_{bf} and F_{br} are the front and rear brake forces, respectively, and $0 < \beta < 1$.

B. BATTERY MODEL

Using an accurate model for the battery pack is critical. A zeroth-order equivalent circuit static model with an internal resistance is used to model each cell in the battery pack [32], [33]. With this approach, the open circuit voltage (OCV) is assumed to vary with the state of charge [32]. The battery pack composed of prismatic 18650 Lithium Nickel Manganese Cobalt Oxide (LNMCO) cells has been chosen [32] to account for the reduction of the weight and increase in the capacity. These cells have high pack density in tight volumes, high capacity and low internal resistance [32]. Using the approach followed by [34], the relationship between OCV and SOC of one NMCO (Nickel Manganese Cobalt Oxide) cell was obtained. The battery pack was sized to ensure the desired range performance to transport the goods from A to D for the given drive cycle. A minimum SOC demand of 15% was assumed, and the energy consumed by auxiliary loads (around 2 – 4% of total energy consumption [35]) was neglected. The detailed derivation is presented next.

The average power delivered by each cell is given by

$$P_c(SOC) = \frac{(V(SOC))^2}{4R_{in}}, \quad (12)$$

where, V represent the cell voltage and R_i represent the cell internal resistance in ohms.

The power demanded at the battery pack at a given SOC can be defined as

$$P_{bat}(SOC) = \frac{P_{mot}}{\eta_m}. \quad (13)$$

Here, $P_{mot} = m_v a(t)v(t) + F_{Rv}(t)v(t)$ is the total power demanded by the hub motors and η_m represents the induction motor efficiency. From this, the number of series and parallel cells (N_s and N_p , respectively) in the battery pack to meet the motor power demand for a range R is given by

$$N_s N_p = \frac{4P_{mot}R}{\eta_m(V(SOC))^2}. \quad (14)$$

Under idle conditions, if one were to ensure the nominal battery pack voltage to match with the nominal

motor voltage ($V_{mot,nom}$),

$$N_s = \lfloor \frac{V_{mot,nom}}{V_c} \rfloor, \quad (15)$$

where, V_c represents the nominal motor voltage and voltage of an individual cell, respectively and $\lfloor \cdot \rfloor$ represents the floor function. From equations (14) and (15), N_p can be computed. Parameters for the vehicle model and battery are taken from [28].

C. PLATOON MODEL

A platoon of autonomous HGVs with one leader and N followers is considered. The vehicles are forced to follow a formation closely following each other at a safe inter-vehicular distance. This makes the vehicles operate as a single unit, allowing them to accelerate/brake together without needing a physical coupling. Following such a formation would improve the road capacity, traffic throughput, road safety, and fuel economy [36]. The fuel economy improvements are from reduced energy consumption due to the reduction in the aerodynamic drag associated with each follower HGV in the platoon. The aerodynamic drag is the resistance offered by the air while moving at a particular speed. As speed increases, the air resistance increases and more energy is required to overcome the drag force. Usually, the air resistance is minimised by streamlining the vehicle design. But in the case of HGVs, due to their large size and frontal area, the aerodynamic drag resistance is prominent and is responsible for more than 50% of total energy consumption during highway operations [37]. Platooning addresses this issue by keeping the vehicles close to each other, thus reducing the effective air resistance, thus saving a significant amount of energy.

For a HGV operating at high speed (usually highway cruise speeds), there is an increased pressure difference between the front and rear end, causing the drag resistance build-up [38]. While in a platoon, the follower HGVs experience drastically reduced pressure differential along their length, thus reducing the aerodynamic drag coefficient. This reduction in drag is directly correlated with the inter-vehicular distances [38]; the closer the vehicles are, the more the drag reduction and vice versa. With this in mind, the following empirical model [38] has been used to represent the drag coefficient reduction for the follower HGVs.

$$C_{Di}(t) = C_{D0}(\gamma_1 d_i(t)^{\gamma_2} + \gamma_3), \quad (16)$$

where, C_{D0} represent the drag coefficient of any individual vehicle (not operating in a platoon formation), $d_i(t)$ is the spacing between the HGVs and the parameters γ_1, γ_2 , and γ_3 are obtained empirically [38]. The spacing between i^{th} and $(i - 1)^{th}$ HGV in the platoon is given by

$$d_i(t) = x_{i-1}(t) - x_i(t). \quad (17)$$

As mentioned above, the inter-vehicular distance between the HGVs is the critical parameter that decides the efficacy and stability of the platoon formation. It is common to keep

the inter-vehicular distance a constant value [39] or allow it to vary according to speed perturbations [23] for increased safety. This work adopts the latter approach by increasing the inter-vehicular distance as speed increases and vice versa, which curtails the chances of rear-end collisions as the HGVs would have more space to stop in case of sudden braking. In this regard, the desired inter-vehicular distance is defined as

$$s_d(t) = s_o + h_i v_i(t), \quad (18)$$

The dependency on velocity is introduced via a scaling factor, h_i , called *time headway*, representing the temporal separation between the rear end of the preceding HGV to the front of the follower HGV about a stationary observer. When time headway magnitudes approach zero, the HGVs are placed closer to each other and might result in collisions. To address this, an additional term, called *stand still spacing* (s_o in equation (18)) is also added to have a non-zero inter-vehicular distance when time headway values near zero or when the HGVs come to a halt/rest. The spacing error between two HGVs can be written as

$$e_i(t) = d_i(t) - s_d(t). \quad (19)$$

In order to maintain a safe/desired inter-vehicular distances at all times and bring the spacing error to zero, an autonomous controller is designed.

D. AUTONOMOUS PLATOON CONTROLLER

Autonomous vehicle operations can improve fuel economy, lower emissions, reduce traffic congestion, and reduce road accidents and related fatalities [40]. The current study considers autonomous HGVs with controllers to maintain the desired speed/position. During the autonomous operation of the HGV, the controller's objective is to track a pre-determined drive cycle saved in the system's memory. The controller attains the goal by eliminating the error between the HGV speed and desired speed by providing the required acceleration/brake inputs. Providing robust control inputs in the presence of external disturbances and different uncertainties is vital for successful autonomous operation. For instance, disturbances such as side winds and sudden jerks due to potholes might be present during HGV operations. Also, there might be uncertainties in road conditions due to rain and snow, which might affect vehicle stability. This necessitates a robust controller to ensure accurate speed tracking and safe HGV operations. The sliding mode control (SMC) technique is a widely accepted robust control strategy that could ensure autonomous system operation in the presence of uncertainties and disturbances [41], [42]. It has proven robust enough to handle external disturbances and different operating uncertainties [23], [28]. Hence, a controller using SMC is used in this study to have fully autonomous and safe HGV operations.

A different approach is used during HGV platooning to ensure a collision-free operation. The lead vehicle uses a

controller for speed tracking, as mentioned above. The follower vehicle's acceleration and brake inputs are computed so that the inter-vehicular distance (gap) between consecutive HGVs remains constant. Ensuring such a criterion, in addition to individual vehicle stability, eliminates the probability of rear-end collisions [28]. Detailed controller design steps are available in [23].

E. ENERGY CONSUMPTION MODEL

One of the most important hurdles of the electrification of HGVs is the increased energy consumption due to the size and weight of the vehicle [14]. While conventional batteries limit the operating range, high-capacity batteries would add to the HGV's weight, adversely affecting the loading capacity. An analysis of the total energy consumption using a close-to-real HGV model would help better understand the challenges and plan efficient policies regarding HGV electrification. For a considered drive cycle, the total energy consumed (E_{dc}) depends on the total power applied to the wheels ($P_{wheel}(t)$)

$$E_{dc} = \int_0^{t_{dc}} P_{wheel}(t) dt, \quad (20)$$

where t_{dc} denotes the drive cycle duration. The total power applied to the wheels depends on the power to overcome the resistive forces and inertial force and is given by

$$P_{wheel}(t) = F_{Rv}(t)v(t) + m_v a(t)v(t), \quad (21)$$

where m_v is the mass of the vehicle, $a(t)$ and $v(t)$ represent the HGV acceleration and speed, respectively with $F_{Rv}(t)$ representing the resistive forces. The aerodynamic drag force, forces due to the rolling resistance at the front and rear wheels, and the force component due to road gradient constitute the resistive forces. At lower speeds, more energy is spent overcoming the rolling resistance and gravity components. But as speed increases, the aerodynamic drag component becomes prominent, and for a HGV cruising at a constant speed, most energy is exhausted on overcoming the air resistance in the form of the aerodynamic drag. Also, the power required to overcome the drag is proportional to the third power of the HGV speed, so even small speed increments would consume more energy. It is logical to compute the energy consumption for only positive values of power. This implies $P_{wheel}(t)$ as presented in Equation (21) should be greater than zero. This implies the acceleration should be greater than $-\frac{F_{Rv}(t)}{m_v}$, and this criterion ensures a positive applied wheel power. Using this method, the total energy consumption for an individual HGV operating individually and in a platoon is computed.

III. RESULTS

As depicted in Figure 2, a scenario where the HGVs transport commodities from warehouse 1 ('A') to warehouse 2 ('D') has been considered. The entire route, labelled as 'A-D', is classified into different sub-sections, 'A-B', 'B-C', and 'C-D'. Sub-sections 'A-B' and 'C-D' represent the side roads (of 2.5 km each) to enter and exit the expressway

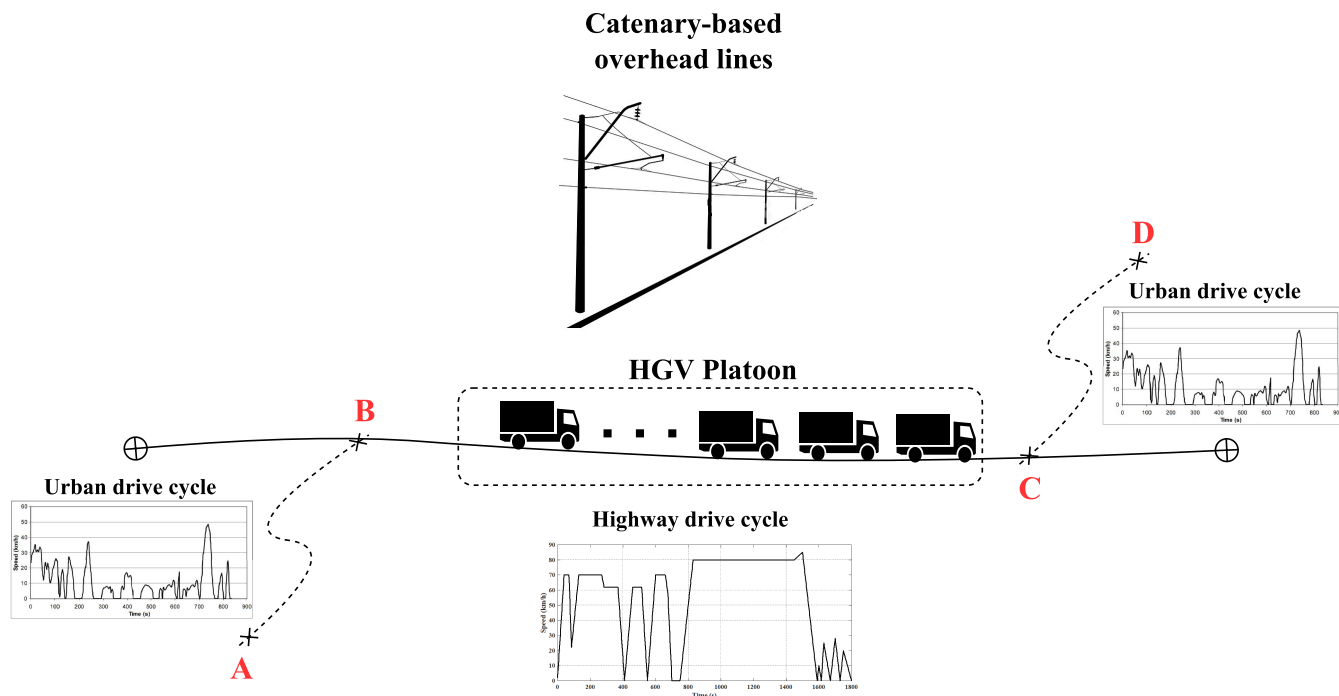


FIGURE 2. Schematic diagram of the considered operating stretch. In stretch AB and CD, the overhead infrastructure is not available. Stretch BC utilizes the overhead line infrastructure to power the HGV. (The figure is not to scale.)

sub-section 'B-C'. The expressway, 'B-C', is assumed to be a longer route of length 75 km with the availability of an electrified stretch with a catenary-based overhead infrastructure. Based on the classification of the roads, two distinct drive cycles, expressed in terms of speed (km/h) versus time, are considered. An in-service drive cycle originally used in [43] has been used for the high-speed expressway subsection 'B-C'. This drive cycle accounts for the speed perturbations to account for the variability of traffic on highways, rather than just a constant speed operation. Whereas the drive cycle 'UG214 HGV08: congested control' proposed by the UK's Department of Transport [44], [45] has been used for the low-speed road sections ('A-B' and 'C-D') with little/no traffic management. The choice of this drive cycle assures the emulation of the limiting operating conditions such as road humps, junctions, and queues of the side roads as claimed in [44].

Research in [46] highlights the impact of the topography variability on the energy consumption and the range of operation of HGVs. As in Figure 3, an uneven elevation profile is used in addition to a level road condition to gauge topography's influence. A representative elevation profile from [43] defines the uneven case in this study.

As envisioned in [3], [47], [48], and [49], electrified HGVs become the greener logistic solution for freight operations. This paper uses a detailed vehicle dynamics-based electric HGV model to emulate the actual operations of class 8 HGVs of 16200 kg (fully laden) on the road. Long-haul operations of such HGVs demand a large battery for greener operations.

Consequently, the gross vehicle weight rating (GVWR) [50] increases and thus the energy consumption. Assuming a limited maximum operating range of 100 km, a 270 kWh [28] lumped battery pack would suffice as the power source [21]. The inclusion of this adds 1220 kg [28] more to the original GVWR. The vehicle and road parameter values used for the study are taken from [28].

This study's detailed mathematical model of the battery electric vehicle (BEV) constitutes longitudinal vehicle and wheel dynamics, nonlinear tyre, electric motor, friction and regenerative brake models, and a robust nonlinear controller. The robust nonlinear controller tracks the overall drive cycle precisely. Three scenarios for the analysis of the considered operation on route 'A-D' with the electric HGV model are:

- **Scenario 1: Exclusive BEV operation** - The HGV is assumed to operate on battery power without utilizing the overhead catenary infrastructure for all time.
- **Scenario 2: BEV operation with Catenary usage** - The power source is switched between an overhead line and a 270 kWh lumped battery pack according to the availability of the overhead infrastructure.
- **Scenario 3: BEV Platooning with Catenary usage** - HGVs are assumed to follow a platoon formation while the power source used is identical to that in **Scenario 2**.

The total energy consumption and battery state of charge (SOC) are determined in each of the above scenarios using the chosen drive cycle and elevation profiles.

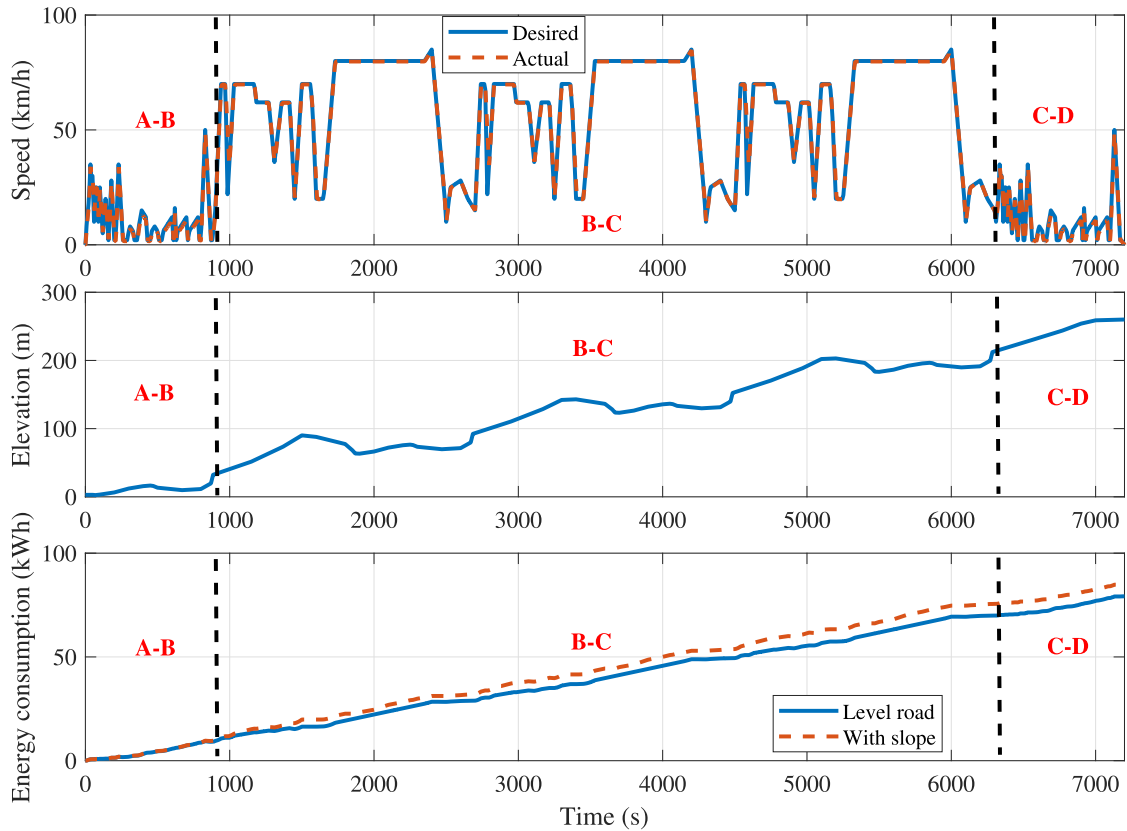


FIGURE 3. Drive cycle tracking profiles, road elevation, and cumulative energy consumption plots for an individual EV travelling from 'A' to 'D'.

A. SCENARIO 1: EXCLUSIVE BEV OPERATION

In this scenario, a 270 kWh battery pack is considered as the power source during the operation. The battery is assumed to be fully charged at warehouse 1, and the vehicle is driven to warehouse 2 following the drive cycle presented in Figure 3. Figure 3 illustrates the speed tracking profiles. Simulations are done for both zero and non-zero elevation profiles to analyse the effect of topography changes on energy consumption. At the end of the operation, operating on a road with the considered elevation profile consumed $\approx 7.3\%$ more energy as compared to that of on a level road. Battery discharges continuously during the trip according to the drive cycle and road conditions.

Figure 4a presents the temporal variation of the SOC for the electric HGV operating in pure battery mode. At the end of section 'A-B', the SOC was found to be $\approx 90\%$, dropping at a rate of $4\%/km$. This is attributed to the increased energy consumption during the repeated acceleration/deceleration cycles in the 'A-B' stretch. During the highway operation, the drop in SOC was improved to $0.8\%/km$ and $0.88\%/km$ for road conditions with zero and non-zero elevation profiles, respectively. At the end of the stretch ('C'), the SOC magnitudes were at 30% and 24.4% for the two considered road topography conditions. The BEV reaches warehouse 2 after consuming another 10% of battery charge while driving through the side road 'C-D'. The HGV is left with only

20% and 14.4% battery charge when it reaches warehouse 2, for level road and a road with slope, respectively, as presented in Figure 4a. The HGV battery has to be plugged into a charging point before planning the next trip.

B. SCENARIO 2: BEV + CATENARY INTEGRATED OPERATION

In this scenario, the HGV utilises the available overhead catenary infrastructure during the stretch 'B-C'. While operating on side roads, the battery powers the HGV and in the availability of the overhead catenary, the HGV utilises a pantograph to connect to the grid and use it as the power source. During the use of catenary, the battery SOC is assumed to remain constant. For the same drive cycle and elevation profiles, as presented in Figure 3, the temporal variation of battery SOC is shown in Figure 4b. The battery powers the HGV while operating on side roads 'A-B' and 'C-D', and the drop in SOC is similar to that in Figure 4a. Since the HGV consumes energy from the grid directly using the overhead catenary infrastructure, it would have $\approx 80\%$ charge even when it reaches warehouse 2. Contrary to the 85.6% usage of the battery charge in pure BEV operation, transport from warehouse 1 to warehouse 2 required only 20% of the battery charge in the present scenario. Though the total energy consumed remains identical, using a grid instead of the battery enhances the potential operation of the HGV because of the

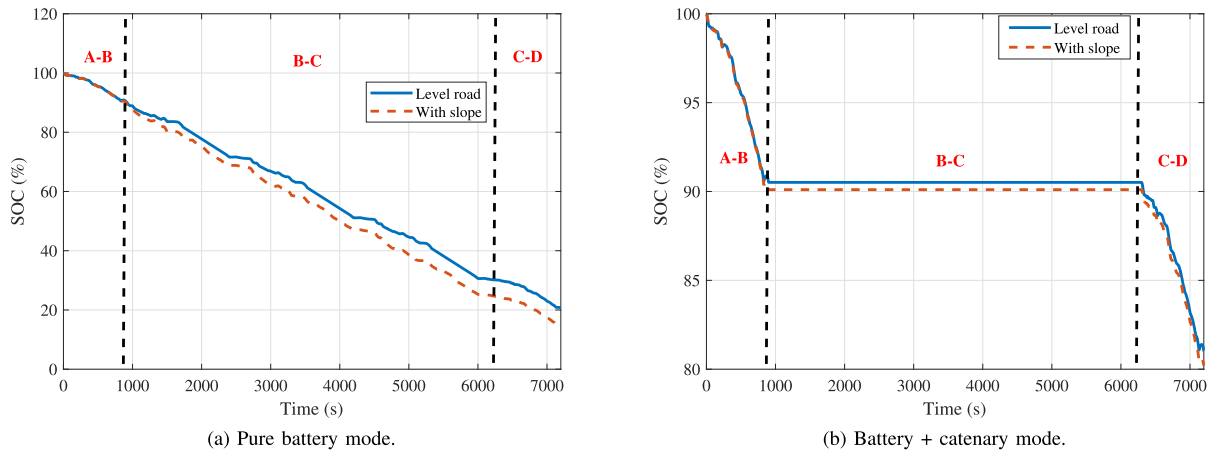


FIGURE 4. State of charge variation for an individual electric HGV.

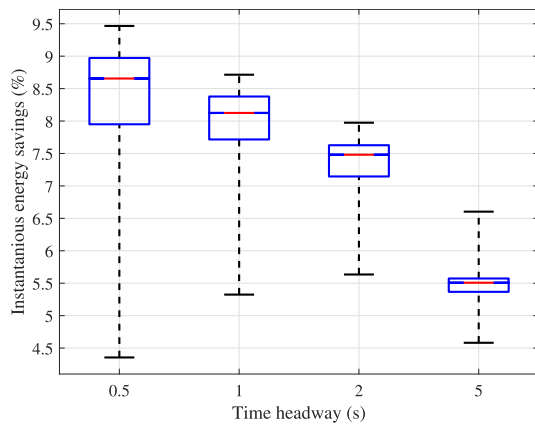


FIGURE 5. Instantaneous energy savings for an individual follower HGV operating in a platoon formation for different time headway magnitudes.

less critical need for an immediate charging of the depleted battery.

C. SCENARIO 3: PLATOONING AT ELECTRIFIED STRETCH 'B-C'

According to research in [26], [28], and [25], platooning of HGVs promises a considerable reduction in energy consumption (up to 10%), and maximum utilisation of the available road infrastructure by reducing congestion and increasing traffic throughput [51]. While operating a vehicle, a significant amount of energy is consumed to overcome the aerodynamic drag force induced by the air resistance to the vehicle motion. The power required to overcome the drag force increases cubically to the vehicle's speed. This component is more prominent for HGVs due to their larger front areas and bluff body shapes [5]. In a platoon, the HGVs will operate at a minimum safe distance from each other, reducing the individual aerodynamic drag force and energy consumption. Hence, the idea here is to analyse the advantages of using such a platoon policy and quantify the reduction in total energy consumption.

A platoon of five autonomous electric HGVs (adhering to the maximum number of vehicles in a platoon limitation as suggested by [52]) with a GVWR of 17420 kg (including battery) is considered. The lead HGV is assumed to be equipped with an autonomous controller for ensuring the drive cycle tracking. A platooning controller provides collision-free operation while maintaining a minimum safe inter-vehicular distance among the follower HGVs. The inter-vehicular distance is defined as a function of the HGV's speed and time headway, and controlling this inter-vehicular distance automatically according to the position and speed of the HGVs avoids collision. In this scenario, the HGVs are assumed to be in a platoon formation during the 'B-C' stretch.

The analysis is done for a constant standstill spacing magnitude of 5 m, and four different time headway magnitudes, 0.5 s, 1 s, 2 s, and 5 s. The instantaneous energy savings in percentage for a follower HGV with an identical drive cycle and elevation profile in Figure 3 for different time headway values are presented in Figure 5. From Figure 5, for the considered drive cycle and operating conditions, each follower HGV in the platoon was found to be having a median (mean) energy savings of 8.66% (8.41%), 8.12% (8.00%), 7.48% (7.37%), and 5.5% (5.47%), for time headway magnitudes of 0.5 s, 1 s, 2 s, and 5 s, respectively. The 25th and 75th percentile values and the maximum and minimum savings for each case are presented. The reduction in energy consumption heavily depends on the drive cycle parameters. For instance, as mentioned before, the aerodynamic drag contribution to the energy consumption is prominent at higher speeds. For a vehicle cruising on a highway with higher speeds, operating in a platoon formation reduces the air resistance, thus saving the energy required to overcome the drag force. Thus, platooning ensures maximum energy savings at higher constant speeds saving up to $\approx 9.5\%$ (Figure 5 for headway magnitude of 0.5 s) during the constant speed cruise phase presented in Figure 3. During low speed operation and recurrent acceleration/deceleration manoeuvres, the energy savings is considerably less (as low as $\approx 5\%$ in Figure 5 for

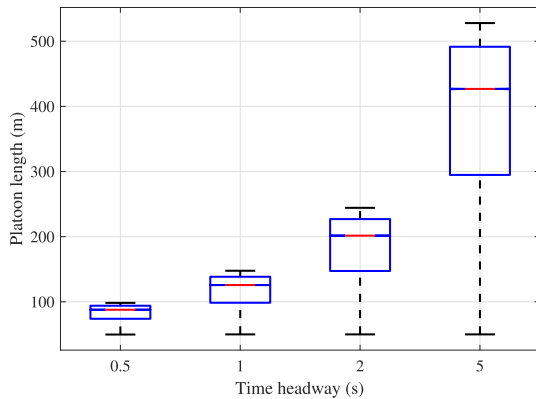


FIGURE 6. Platoon length variation as a measure of road utilization for different time headway magnitudes.

headway magnitude of 0.5 s) compared to that of constant speed operation. Nonetheless, adoption of platooning ensures overall energy savings as presented in Figure 5. Time headway directly impacts the energy saved while operating in a platoon formation. Shorter time headway magnitudes imply closely spaced vehicles, thus reducing the aerodynamic drag on the HGVs considerably, reducing the energy required to overcome the same. This reduction is reflected as the energy savings in Figure 5. From the presented results, one could observe a steady decline in the mean energy savings from 8.41% to 5.47% for a time headway increase from 0.5 s to 5 s. Also, the total energy savings for a HGV in a platoon formation with a time headway magnitude of 5 s is found to be $\approx 1/3^{rd}$ of that of an HGV in a platoon with a headway magnitude of 0.5 s. If headway is further increased to higher values (15 s for the presented work), the energy savings would be insignificant, and total energy consumption would be comparable to that of an individual HGV operation (as presented in Figure 3).

In addition to saving energy, platooning also improves the available infrastructure/road utilisation by operating as a compact unit, thus saving space and improving traffic throughput. Consequent advantages are, to name a few, increased road capacity, reduced congestion and safe and collision-free operations. The variation of platoon length, computed as the cumulative value of the HGV length and inter-vehicular distances, for different time headway values is presented in Figure 6. In the considered case, for a headway magnitude of 0.5 s, the platoon of five HGVs covers the highway as a compact unit with a mean length of 83.23 m. This would drastically improve the traffic flow throughput and reduces congestion by reducing the chances of other vehicles entering the HGV lane. As headway magnitude increases, the inter-vehicular distance increases, and the platoon gets more spread out, as shown in Figure 6. Increasing the headway and, in turn, the inter-vehicular distance may not be desired, but may be necessary to avoid collisions and ensure a safe operation. Still, from economic and traffic efficiency perspectives, HGV platooning is a better solution for logistic transport than individual HGV operations. However, implementation of on-road platooning should consider safety aspects that

may lead to collision between the HGVs, especially in an autonomous capacity. Factors such as vehicle to vehicle communication delays and packet-drops, and on-road perturbations need to be considered and suitably addressed for safe platooning. The active safety systems in HGVs should be robust enough to avoid any possible mishaps. The recent promising advancements in autonomous HGV platooning could potentially address these concerns and be relied upon for safe platoon operations [24], [53], [54].

IV. DISCUSSIONS

HGV operators prefer overnight charging [55] using typical AC fast chargers up to 22 kW for purely economic reasons. The fleet operators can use less expensive, commercially available chargers and can install them/use third-party infrastructure. It is possible to improve the charging time by installing DC fast charges, but it would cost ≈ 10 times the cost of conventional AC chargers [55]. An increased capital expense from installing exclusive DC fast-charging stations might impede the immediate use of electric HGVs from an operator's perspective. Adopting overnight charging would cause significant downtime, adversely affecting logistic productivity and the cost-to-benefit ratio while using an electric HGV. Yet another factor that could hinder the use of battery-operated HGVs could be the need for battery replacements. A typical Li-ion battery costs around 300 \$/kWh and lasts approximately 1000 charging cycles [14] with an optimistic price projection of 100 \$/kWh by 2025 [14]. The need for repeated charging after each operation necessitates the need for much faster battery replacement. Using overhead catenary power allows the operator to avoid increased battery expenses. It is also common to use much smaller batteries along with the catenary operation, which would reduce battery expenses and weight optimisation. Since the battery and associated costs are about 40-60% of total electric HGV capital expenditure [55], any attempt to reduce the battery cost would make the electric HGV cheaper and more affordable.

As an exemplary pilot study to critically gauge the potential of sustainable transport solutions and recommendations, a realistic scenario of an electric HGV transporting commodities between two warehouses was considered. The viability of operating a battery-powered electric HGV individually and in a platoon formation, with and without overhead catenary support, is analysed. When used as an individual unit, it is recommended to supplement the HGV with direct grid power from the overhead catenary line (whenever available). For a trip to the second warehouse with the considered elevation profile and drive cycle, the battery in a battery-powered HGV discharges down to $\approx 14.4\%$, whereas integrating with an overhead catenary preserves the charge up to $\approx 80\%$. This could impact the logistics sector in multiple ways. For instance, an HGV with pure battery power can not start a new trip without recharging. This study reveals that an HGV equipped with an overhead catenary drawing electric power over particular highway segments (corresponding to 'B-C' part of the drive cycle as shown in Figure 3) can cover

approximately four times the distance that of a pure battery-operated HGV. Integrating a catenary and using grid power as a supplementary power source can alleviate the range anxiety problem, especially in electric HGVs. On the other hand, it is also possible to reduce the battery size, which can in turn have significant impact on the overall cost. It could be possible to operate HGVs with smaller, and more economical batteries, that can be used on roads where catenary infrastructure is not available (for instance sections 'A-B' and 'C-D' in Figure 3).

Platooning presents an option to encourage the electrification of HGVs for logistic transport. Operating in a platoon formation reduces the energy consumption per HGV considerably. For instance, for the considered scenario and drive cycle, five operating HGVs consume a total energy of 425 kWh, with each HGV consuming around 1.06 kWh/km. If HGVs operate in a platoon, considering the best and worst case scenarios analysed, a unique follower HGV consumes approximately 0.95 kWh/km and 1 kWh/km, respectively, with a combined energy consumption (for five HGVs) of 395.5 kWh. These savings are more significant during constant-speed highway operations. At higher speeds, most energy is consumed to overcome the aerodynamic drag force acting on the HGVs and platooning reduces the drag to minimise energy loss and operating cost. If one considers an electricity cost of 52 p/kWh [56], then for the considered scenario, one can ensure a reduction in the price of up to 5.72 p/km in electricity charges for operating an individual HGV in a platoon formation. So, adopting a similar approach for long-haul freight transport incorporating more HGVs would significantly reduce operating costs.

V. CONCLUSION

Economically viable and technologically adaptable decarbonisation methods are vital for a sustainable future. The proposed research ascertains the expected outcomes from the prospective implementation of some of the methodologies for decarbonisation using a detailed simulation of the vehicle dynamics. The simulation framework in this paper can simulate close-to-real scenarios to appreciate and analyse different aspects of using autonomous electrified HGVs as a cleaner logistic solution. Based on the detailed analysis, it has been observed that platooning of electrified HGVs, powered from overhead catenary cables, would be a sustainable solution for long-haul road freight transportation. This could be seen as an immediate solution to boost truck electrification without compromising on the payload capacity and range of operation of long-haul trucks for efficient freight movement.

REFERENCES

- [1] Department of Transport. (2021). *Transport and Environment Statistics 2021 Annual Report*. Accessed: Nov. 10, 2022. [Online]. Available: https://assets.publishing.service.gov.uk/government/uploads/system/uploads/attachment_data/file/984685/transport-and-environment-statistics-2021.pdf
- [2] M. Kumar, Z. Shao, C. Braun, and A. Bandivadekar, "Decarbonizing India's road transport: A meta-analysis of road transport emissions models," *Int. Council Clean Transp.*, pp. 1–34, May 2022. [Online]. Available: <http://www.indiaenvironmentportal.org.in/files/file/Meta%20study%20India%20transport.pdf>
- [3] M. Moutak, N. Lutsey, and D. Hall, "Transitioning to zero-emission heavy-duty freight vehicles," *Int. Council Clean Transp.*, 2017.
- [4] M. Juhala, "Improving vehicle rolling resistance and aerodynamics," in *Alternative Fuels and Advanced Vehicle Technologies for Improved Environmental Performance*. Sawston, U.K.: Woodhead Publishing, 2014, pp. 462–475.
- [5] Z. Mohamed-Kassim and A. Filippone, "Fuel savings on a heavy vehicle via aerodynamic drag reduction," *Transp. Res. D, Transp. Environ.*, vol. 15, no. 5, pp. 275–284, Jul. 2010.
- [6] O. Golbasi and E. Kina, "Haul truck fuel consumption modeling under random operating conditions: A case study," *Transp. Res. D, Transp. Environ.*, vol. 102, Jan. 2022, Art. no. 103135.
- [7] A. Alonso-Villar, B. Davíðsdóttir, H. Stefánsson, E. I. Ásgeirsson, and R. Kristjánsson, "Technical, economic, and environmental feasibility of alternative fuel heavy-duty vehicles in Iceland," *J. Cleaner Prod.*, vol. 369, Oct. 2022, Art. no. 133249.
- [8] D. Mehlh, H. Woodward, T. Oxley, M. Holland, and H. ApSimon, "Electrification of road transport and the impacts on air quality and health in the UK," *Atmosphere*, vol. 12, no. 11, p. 1491, Nov. 2021.
- [9] R. Stoshansi and P. Denholm, "Emissions impacts and benefits of plug-in hybrid electric vehicles and vehicle-to-grid services," *Environ. Sci. Technol.*, vol. 43, no. 4, pp. 1199–1204, Feb. 2009.
- [10] E. Çabukoglu, G. Georges, L. Küng, G. Pareschi, and K. Boulouchos, "Fuel cell electric vehicles: An option to decarbonize heavy-duty transport? Results from a Swiss case-study," *Transp. Res. D, Transp. Environ.*, vol. 70, pp. 35–48, May 2019.
- [11] B. Kin, M. Hopman, and H. Quak, "Different charging strategies for electric vehicle fleets in urban freight transport," *Sustainability*, vol. 13, no. 23, p. 13080, Nov. 2021.
- [12] T. Earl, L. Mathieu, S. Cornelis, S. Kenny, C. C. Ambel, and J. Nix, "Analysis of long haul battery electric trucks in EU," in *Proc. Commercial Vehicle Workshop*, 2018, pp. 1–22.
- [13] M. Zähringer, S. Wolff, J. Schneider, G. Balke, and M. Lienkamp, "Time vs. capacity—The potential of optimal charging stop strategies for battery electric trucks," *Energies*, vol. 15, no. 19, p. 7137, Sep. 2022.
- [14] B. Nykvist and O. Olsson, "The feasibility of heavy battery electric trucks," *Joule*, vol. 5, no. 4, pp. 901–913, Apr. 2021.
- [15] C. A. García-Vázquez, F. Llorens-Iborra, L. M. Fernández-Ramírez, H. Sánchez-Sainz, and F. Jurado, "Comparative study of dynamic wireless charging of electric vehicles in motorway, highway and urban stretches," *Energy*, vol. 137, pp. 42–57, Oct. 2017.
- [16] I. Mareev and D. Sauer, "Energy consumption and life cycle costs of overhead catenary heavy-duty trucks for long-haul transportation," *Energies*, vol. 11, no. 12, p. 3446, Dec. 2018.
- [17] L. Netzer, D. Wöss, T. Märzinger, W. Muller, and T. Pröll, "Impact of an E-highway on the required battery capacities and charging infrastructure for cargo transport with E-trucks on the basis of a real use case," *Energies*, vol. 15, no. 19, p. 7102, Sep. 2022.
- [18] M. Wolek, M. Wolanski, M. Bartłomiejczyk, O. Wyszomirski, K. Grzelec, and K. Hebel, "Ensuring sustainable development of urban public transport: A case study of the trolleybus system in Gdynia and Sopot (Poland)," *J. Cleaner Prod.*, vol. 279, Jan. 2021, Art. no. 123807.
- [19] *Ehighway—Solutions for Electrified Road Freight Transport*, Siemens, Germany, 2021.
- [20] A. Scherrer and U. Burghard, "Social acceptance of catenary hybrid trucks in Germany—first results from the accompanying research of eWayBW," in *Proc. 3rd Electric Road Syst. Conf.*, 2019, pp. 1–5.
- [21] D. Ainalis, C. Thorne, and D. Cebon, "Decarbonising the UK's long-haul road freight at minimum economic cost," Centre Sustain. Road Freight, Cambridge, U.K., White Paper CUED/C-SRF/TR17, 2020.
- [22] C. de Saxe, D. Ainalis, J. Miles, P. Greening, A. Gripton, C. Thorne, and D. Cebon, "An electric road system or big batteries: Implications for UK road freight," doi: [10.2139/ssrn.4194379](https://doi.org/10.2139/ssrn.4194379).
- [23] K. B. Devika, V. R. S. Yellapantula, and S. C. Subramanian, "A dynamics-based adaptive string stable controller for connected heavy road vehicle platoon safety," *IEEE Access*, vol. 8, pp. 209886–209903, 2020.
- [24] X. Guo, J. Wang, F. Liao, and R. S. H. Teo, "Distributed adaptive integrated-sliding-mode controller synthesis for string stability of vehicle platoons," *IEEE Trans. Intell. Transp. Syst.*, vol. 17, no. 9, pp. 2419–2429, Sep. 2016.
- [25] M. P. Lammert, A. Duran, J. Diez, K. Burton, and A. Nicholson, "Effect of platooning on fuel consumption of class 8 vehicles over a range of speeds, following distances, and mass," Nat. Renew. Energy Lab. (NREL), Golden, CO, USA, Tech. Rep. NREL/CP-5400-62348, 2014.
- [26] A. Alam, B. Besselink, V. Turri, J. Mårtensson, and K. H. Johansson, "Heavy-duty vehicle platooning for sustainable freight transportation: A cooperative method to enhance safety and efficiency," *IEEE Control Syst. Mag.*, vol. 35, no. 6, pp. 34–56, Dec. 2015.

- [27] H. Pacejka, *Tire and Vehicle Dynamics*. Elsevier, 2005.
- [28] K. B. Devika, G. Rohith, and S. C. Subramanian, "String stable control of electric heavy vehicle platoon with varying battery pack locations," *J. Vibrat. Control*, vol. 28, nos. 5–6, pp. 577–592, Mar. 2022.
- [29] K. V. Subramaniyam and S. C. Subramanian, "Impact of regenerative braking torque blend-out characteristics on electrified heavy road vehicle braking performance," *Vehicle Syst. Dyn.*, vol. 59, no. 2, pp. 269–294, 2019.
- [30] N. Sridhar, K. V. Subramaniyam, S. C. Subramanian, G. Vivekanandan, and S. Sivaram, "Model based control of heavy road vehicle brakes for active safety applications," in *Proc. 14th IEEE India Council Int. Conf. (INDICON)*, Dec. 2017, pp. 1–6.
- [31] M. Ehsani, Y. Gao, S. Longo, and K. Ebrahimi, *Modern Electric, Hybrid Electric, and Fuel Cell Vehicles*. CRC Press, 2018.
- [32] F.-A. LeBel, L. Pelletier, P. Messier, and J. P. Trovao, "Battery pack sizing method-case study of an electric motorcycle," in *Proc. IEEE Vehicle Power Propuls. Conf. (VPPC)*, Mar. 2018, pp. 1–6.
- [33] S. Suriyamoorthy, S. Gupta, D. P. Kumar, and S. C. Subramanian, "Analysis of hub motor configuration and battery placement on ride comfort of electric trucks," in *Proc. IEEE Vehicle Power Propuls. Conf. (VPPC)*, Oct. 2019, pp. 1–6.
- [34] C. Zhang, J. Jiang, L. Zhang, S. Liu, L. Wang, and P. Loh, "A generalized SOC-OCV model for lithium-ion batteries and the SOC estimation for LNMCO battery," *Energies*, vol. 9, no. 11, p. 900, Nov. 2016.
- [35] M. Khodabakhshian, L. Feng, S. Börjesson, Ö. Lindgärde, and J. Wikander, "Reducing auxiliary energy consumption of heavy trucks by onboard prediction and real-time optimization," *Appl. Energy*, vol. 188, pp. 652–671, Feb. 2017.
- [36] J. Leech, G. Whelan, M. Bhajji, M. Hawes, and K. Scharring, "Connected and autonomous vehicles—the UK economic opportunity," KPMG, U.K., Tech. Rep., 2015. [Online]. Available: <https://assets.kpmg.com/content/dam/kpmg/pdf/2015/04/connected-and-autonomous-vehicles.pdf#:~:text=%E2%80%A2The%20overall%20economic%20and%20social%20benefit%20of%20connected,25%2C000%20of%20which%20would%20be%20in%20automotive%20manufacturing>
- [37] R. McCallen, "Progress in reducing aerodynamic drag for higher efficiency of heavy duty trucks (class 7–8)," Lawrence Livermore Nat. Lab. (LLNL), Livermore, CA, USA, Tech. Rep., 1999. [Online]. Available: <https://www.osti.gov/servlets/purl/771211>
- [38] A. A. Hussein and H. A. Rakha, "Vehicle platooning impact on drag coefficients and energy/fuel saving implications," 2020, *arXiv:2001.00560*.
- [39] D. Swaroop, J. K. Hedrick, C. C. Chien, and P. Ioannou, "A comparison of spacing and headway control laws for automatically controlled vehicles," *Vehicle Syst. Dyn.*, vol. 23, no. 1, pp. 597–625, 1994.
- [40] J. M. Anderson, K. Nidhi, K. D. Stanley, P. Sorensen, C. Samaras, and O. A. Oluwatola, *Autonomous Vehicle Technology: A Guide for Policymakers*. Rand Corporation, 2014.
- [41] J. Y. Hung, W. Gao, and J. C. Hung, "Variable structure control: A survey," *IEEE Trans. Ind. Electron.*, vol. 40, no. 1, pp. 2–22, Feb. 1993.
- [42] Y. Shtessel, *Sliding Mode Control and Observation*, vol. 10. New York, NY, USA: Springer, 2014.
- [43] A. K. Madhusudhanan, X. Na, and D. Cebon, "A computationally efficient framework for modelling energy consumption of ICE and electric vehicles," *Energies*, vol. 14, no. 7, p. 2031, Apr. 2021.
- [44] J. Green and T. Barlow, *Traffic Management and Air Quality: Realistic Driving Cycles for Traffic Management Schemes*. Crowthorne, U.K.: TRL, 2004.
- [45] T. Barlow, S. Latham, I. McCrae, and P. Boulter, "A reference book of driving cycles for use in the measurement of road vehicle emissions: Version 3," IHS, Bracknell, U.K., 2009.
- [46] R. G. K. B. Devika, P. P. Menon, and S. C. Subramanian, "An adaptive time-headway policy for lower energy consumption in autonomous vehicle platoons," in *Proc. Eur. Control Conf. (ECC)*, Jul. 2022, pp. 1734–1739.
- [47] E. Çabukoglu, G. Georges, L. Kung, G. Pareschi, and K. Boulouchos, "Battery electric propulsion: An option for heavy-duty vehicles? Results from a Swiss case-study," *Transp. Res. C, Emerg. Technol.*, vol. 88, pp. 107–123, Mar. 2018.
- [48] K. Forrest, M. M. Kinnon, B. Tarroja, and S. Samuelsen, "Estimating the technical feasibility of fuel cell and battery electric vehicles for the medium and heavy duty sectors in California," *Appl. Energy*, vol. 276, Jan. 2020, Art. no. 115439.
- [49] H. Liimatainen, O. van Vliet, and D. Aplyn, "The potential of electric trucks—An international commodity-level analysis," *Appl. Energy*, vol. 236, pp. 804–814, Mar. 2019.
- [50] D. Smith, "Medium- and heavy-duty vehicle electrification: An assessment of technology and knowledge gaps," Oak Ridge National Lab. (ORNL), Oak Ridge, TN, USA, Tech. Rep. ORNL/SPR-2020/7, 2020.
- [51] O. E. Gungor, R. She, I. L. Al-Qadi, and Y. Ouyang, "One for all: Decentralized optimization of lateral position of autonomous trucks in a platoon to improve roadway infrastructure sustainability," *Transp. Res. C, Emerg. Technol.*, vol. 120, Nov. 2020, Art. no. 102783.
- [52] Ricardo, TRL, and TTR. (2014). *Heavy Vehicle Platoons on UK Roads: A Feasibility Study*. Accessed: Nov. 6, 2022. [Online]. Available: https://assets.publishing.service.gov.uk/government/uploads/system/uploads/attachment_data/file/637361/truck-platooning-uk-feasibility-study.pdf
- [53] Z. Qiang, L. Dai, B. Chen, and Y. Xia, "Distributed model predictive control for heterogeneous vehicle platoon with inter-vehicular spacing constraints," *IEEE Trans. Intell. Transp. Syst.*, vol. 24, no. 3, pp. 3339–3351, Mar. 2023.
- [54] K. B. Devika, G. Rohith, and S. C. Subramanian, "Heavy road vehicle platoon control considering brake fade with adaptive mass and road gradient estimation," *IEEE Access*, vol. 10, pp. 107227–107241, 2022.
- [55] *Why Most Etrucks Will Choose Overnight Charging*. Accessed: Jul. 1, 2022. [Online]. Available: <https://www.mckinsey.com/industries/automotive-and-assembly/our-insights/why-most-etrucks-will-choose-overnight-charging>
- [56] (2022). *Gas and Electricity Prices in the Non-Domestic Sector*. Accessed: Jun. 1, 2022. [Online]. Available: <https://www.gov.uk/government/statistical-data-sets/gas-and-electricity-prices-in-the-non-domestic-sector>



G. ROHITH received the Ph.D. degree in aerospace engineering from the Indian Institute of Technology Madras, India. He is currently a Control Systems Engineer with Orbital Astronautics, Oxfordshire, U.K. His research interests include the dynamics and control of automotive and aerospace systems and satellite attitude determination and control.



K. B. DEVIKA is currently a Lecturer of mechanical engineering with the Faculty of Environment, Science and Economy, University of Exeter, U.K. She is also an Adjunct Faculty with the Department of Engineering Design, Indian Institute of Technology Madras, India. Her research interests include the control of automotive and transportation systems, sustainable road freight transportation, clean mobility, and sliding mode control.



PRATHYUSH P. MENON is currently an Associate Professor of control systems with the Faculty of Environment, Science and Economy, University of Exeter, U.K., where he is also the Deputy Director of the Centre for Future Clean Mobility. His current research interests include control, sliding mode observers, multiagent systems, energy networks, optimization, and simulation-based robustness analysis and uncertainty quantification. He has authored 100 refereed articles in these areas, including 40 journal publications.



SHANKAR C. SUBRAMANIAN (Senior Member, IEEE) received the Ph.D. degree from Texas A&M University, USA. He is currently a Professor and a V. Ramamurti Faculty Fellow with the Department of Engineering Design, Indian Institute of Technology Madras, Chennai, India. His research interest includes dynamics and control with applications to automotive and transportation systems.